Relative Navigation Scheme of the Final Approach Phase for Space Robot

Bibo Guo, Bing Liang, Cheng Li
The Institute of Space Intelligent System
Harbin Institute of Technology
Harbin, P.R.China
bbguo@robotsat.com, bliang@robotsat.com
cli@robotsat.com

Wenyi Qiang
Astronautics School
Harbin Institute of Technology
Harbin, P.R.China
wyqiang@hit.edu.cn

***Abstract*—Space robotic relative navigation is one of the key technologies for on-orbital tracking and approaching. It can supplies the relative position and attitude information of target spacecraft. In this paper, a relative navigation scheme for the final approach phase was proposed, with the target spacecraft information measured by optical sensor. Firstly, we designed a linear Kalman filter which is used to relative navigation with constant gain, combining the relative motion dynamics (between two spacecrafts) with the measure principle of optimal sensor. The second, the relative navigation algorithm was improved by the coordinate transformation and the devices calibration, So the effects on the accuracy resulting from the attitude bias of spacecraft and the mounted errors of the optical sensors were largely reduced. Then, the dynamic performance of the filter was theoretically analyzed according to the positions of its poles. At last, a hardware-in-loop test-bed was introduced, on which the navigation algorithm was evaluated. The experiment results verified the developed scheme.**

***Keywords*—space robot, relative navigation, optical sensor, hardware-in-loop simulation**

I. INTRODUCTION

An unmanned free-flying space robot which is able to maintain precise relative position with target can serve many purposes, such as on orbit inspection and repair. The Japanese ETS-VII, the first real free-flying space robot system, demonstrated the rendezvous and docking (RVD) and space robotic (RBT) technologies [1]. Recently, the Orbital Express system, sponsored and led by the Defense Advanced Research Projects Agency (DARPA), validated on-orbit satellite servicing technologies [2]. In order to approaching the target spacecraft in meter-level, the precise relative navigation in centimeter-level is necessary. Many possible technologies have been suggested for achieving this type of precision navigation at extremely close ranges. For example, differential GPS and laser finder range both show promise in certain application, but also have drawbacks [3]. The differential GPS solution would be susceptible to extreme muti-path errors due to the very close proximity of space robot to the target spacecraft. The laser finder need cooperates with other sensor because of the only range information. An effective measure method is fixing optical sensor on space robotic, and some known geometry position markers are fixed on target spacecraft, the optics sensor may compute the accurate relative information by images of markers. A Proximity Sensor (PXS) was used by ETS-VII. Target spacecraft installed a 3-point alignment marker, and a camera with black/white CCD was fixed on chase spacecraft. After screening the marker, the onboard video data processing calculate position and attitude of the alignment marker using relative position of three white circle image of the marker in the video data. The Advanced Video Guidance Sensor (AVGS) was installed on "Orbital Express". The AVGS consists of two parts: the sensor and the target. The sensor was fixed on ASTRO (Chase spacecraft), and the target was fixed on NextSat (target spacecraft). The AVGS operated on a fairly simple theory-the tracking of spots on a known target. By tracking only spots, a large amount of image processing understanding is avoided, and since the spots occupy known position on the target, the sensor can easily determine relative position and attitude data based on centroids of the spots [4].

To date, based on optical measure information, lots of researches have been done about the relative navigation algorithm [5-8]. For example, Texas A&M University and the State University of New York researched a vision-base navigation (VISNAV) system together, the sensor is made up of a Position Sensing Diode (PSD) placed in the focal plane of a wide angle lens. In order to achieve a selective or "intelligent" vision, the target was composed by LED (beacon). The relative position and Attitude could be obtained via Line-of-Sight vectors. The main navigation algorithm was extended Kalman Filter. The relative position and linear velocity observer had been proven to meet quantitive convergence using a contraction mapping analysis. N.K.Philip used fixed gain observers to estimate the position and attitude, and analyzed the sensitivity of different parameter one the estimator.

In this paper, a relative navigation scheme for the final approach phase was proposed, with the target spacecraft information measured by optical sensor. The organization of the paper proceeds as follows. Firstly, the on orbit relative motion dynamics is given. Then, the observation equations are derived, following by series of coordinate transformation and approximate disposal. Next, a constant gain linear Kalman filter used to relative navigation is designed after considering space robot little computation capability, and the dynamic performance of the filter was theoretically analyzed according to the positions of its poles. Next, a hardware-in-loop test bed

978-1-4244-1676-9/08 /$25.00 ©2008 IEEE

with optical sensor system is introduced. Finally, simulation results are presented.

II. RELATIVE POSITION OBSERVATION EQUATION

The guidance and control schemes for the final approach phase require precise information about the position parameters of the target spacecraft relative to space robot. Using CCD camera, optical sensor screens the images of markers which are fixed on the surface of target spacecraft, the correspondence between markers on the target spacecraft and their respective images obtained from the optical sensor are used to estimate the relative attitude and position parameters. Fig. 1 shows space robot relative measure. After obtaining the relative parameters, it's possible to compute the accurate relative navigation result. In this paper, we discuss the relative position navigation mainly.

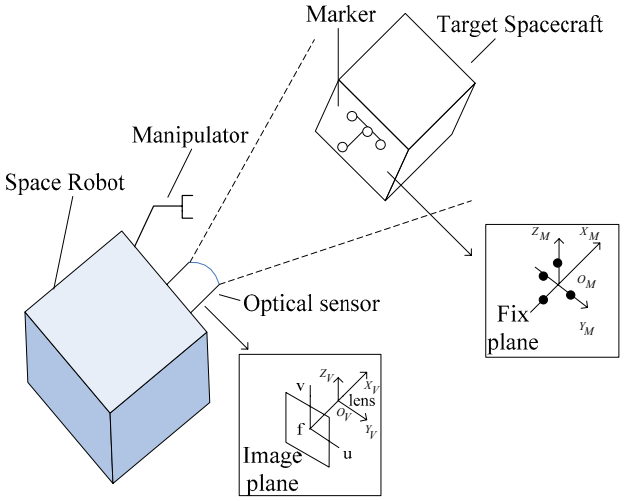

Figure 1. Space robot relative measure

Six frames are used to describe the orientation and position of the space robot and the target spacecraft. The first two, denoted by $O_{Co}X_{Co}Y_{Co}Z_{Co}$ and $O_{Mo}X_{Mo}Y_{Mo}Z_{Mo}$, are space robot and target spacecraft LVLH frame, and the origins are fixed on spacecraft mass centers respectively. The second two, denoted by $O_{Cb}X_{Cb}Y_{Cb}Z_{Cb}$ and $O_{Mb}X_{Mb}Y_{Mb}Z_{Mb}$, are fixed on the bodies of two spacecrafts. LVLH frame is identical with body one when earth pointing bias is zero. The fifth frame, denoted by $O_VX_VY_VZ_V$, is fixed on the optical sensor, where X_V is identical with optics axis and pointing to target. The last one, denoted by $O_MX_MY_MZ_M$, is fixed on the marker, where the fix plane of the marker is located. Fig. 1 shows the optical sensor frame and the marker frame. Fig. 2 shows the LVLH frames. In Fig. 2, some position vectors are defined at the same time. $\boldsymbol{\rho}_C$ is the vector from space robot mass center to sensor center, $\boldsymbol{\rho}_{mes}$ is the vector from sensor center to marker center, $\boldsymbol{\rho}_M$ is the vector from marker center to target spacecraft mass center, and $\boldsymbol{\rho}$ is the vector from space robot mass center to target spacecraft mass center. ρ, ρ_c, ρ_{mes} and ρ_M express the value in target satellite LVLH frame. It gives the following relation

$$\rho = \rho_C + \rho_{mes} + \rho_M \tag{1}$$

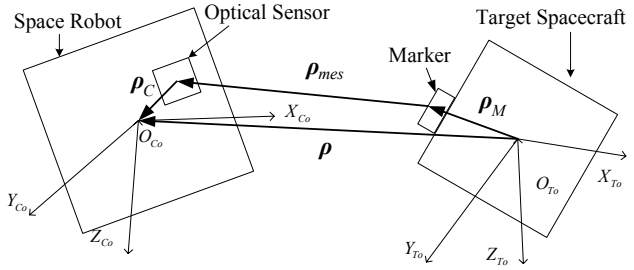

Figure 2. The coordinates and the geometry relationship

At first, we define some variables. R_{To} and V_{To} express the relative position and velocity of two spacecraft mass centers in LVLH frame of target spacecraft. C_{To_Co}, C_{Co_Cb}, C_{Cb_V} and C_{To_Tb} express the direction cosine respectively. For example C_{B_A} is the direction cosine from A frame to B .Mark of $\cdot|_V$ denotes the vector value in V frame. s is defined as the optical sensor measure noise. Y is measure output value, and $Y = \rho_{mes}|_V + s$, $R_{To} = \rho|_{To}$, $V_{To} = \left.\frac{d\rho}{dt}\right|_{To}$, system state value $X = [R_{To}; V_{To}]^T$.

Projected to target spacecraft LVLH frame, (1) can be re-written as follows:

$$(\rho_{mes} - s)|_{To} = \rho|_{To} - \rho_C|_{To} - \rho_M|_{To} \tag{2}$$

Let:

$$\begin{aligned} Y_{new} = {} & C_{To\_Co} \cdot C_{Co\_Cb} \cdot C_{Cb\_V} \cdot \rho_{mes}|_V + \\ & C_{To\_Co} C_{Co\_Cb} \cdot \rho_C|_{Cb} + C_{To\_Tb} \cdot \rho_M|_{Tb} \sqrt{b^2 - 4ac} \end{aligned} \tag{3}$$

$$s_{new} = C_{To\_Co} \cdot C_{Co\_Cb} \cdot C_{Cb\_V} \cdot s|_V \tag{4}$$

The following equations can be obtained by a series of transformation

$$Y_{new} = \rho|_{To} + s_{new} \tag{5}$$

In (3), C_{To_Co} approximates unit matrix because of spacecrafts little relative distance. C_{Cb_V} is known as a certain value, and C_{Co_Cb} can be obtained via space robot 3-axis attitude. C_{To_Tb} is the only unknowable by space robot. Considering target spacecraft little attitude bias to orbit frame, we regard C_{To_Tb} as unit matrix approximately. s_{new} is obtained from $s|_V$ via a series of little attitude transformation, so they has alike statistic characteristic.

The new measure equations can be re-written as follows:

$$Y_{new} = H \cdot X + s_{new} \tag{6}$$

Where $H = \begin{bmatrix} I_{3\times3} \\ 0_{3\times3} \end{bmatrix}$.

III. SPACECRAFT RELATIVE MOTION DYNAMICS MODEL

From basic Kepler orbit theory, the motion equations of space robot and target spacecraft are referenced with the same inertial frame. The dynamics equations are obtained:

$$\ddot{\boldsymbol{r}}_C + \frac{Gm_e(\boldsymbol{r}_M + \boldsymbol{\rho})}{\left\|\boldsymbol{r}_M + \boldsymbol{\rho}\right\|^3} = \boldsymbol{a}_T \tag{7}$$

$$\ddot{\boldsymbol{r}}_M + \frac{Gm_e\boldsymbol{r}_M}{\left\|\boldsymbol{r}_M\right\|^3} = \boldsymbol{a}_M \tag{8}$$

Where G is the universal constant of gravitation, and m_e is the mass of the Earth.

$$\boldsymbol{\rho} = \boldsymbol{r}_M - \boldsymbol{r}_C \tag{9}$$

Taking derivatives with respect to the inertial frame, the following equation is obtained

$$\ddot{\boldsymbol{\rho}} = -\mu_e\left(\frac{\boldsymbol{r}_M + \boldsymbol{\rho}}{\left\|\boldsymbol{r}_M + \boldsymbol{\rho}\right\|^3} - \frac{\boldsymbol{r}_M}{\left\|\boldsymbol{r}_M\right\|^3}\right) \Delta\boldsymbol{a} \tag{10}$$

Where $\mu_e \equiv Gm_e$. The quantity $\Delta\boldsymbol{a} = \boldsymbol{a}_C - \boldsymbol{a}_M$ is the orbit control value and differential disturbance between both spacecrafts, it collects the higher order gravitational potential terms(J2,J3,etc.), and the nonconservative forces (such as drag, solar pressure, etc. al) applied to the spacecrafts [9].

Considering near circular orbit and little relative distance, the differential equation for the relative navigation problem, which is described by (9), can be simplified if an appropriate reference system, other than the inertial frame, is used to express the relative position and velocity vectors. The simplified equation is named as Clohessy-Wiltshire (C-W) equations.

$$\begin{cases} \ddot{x} = a_x + 2\omega\dot{z} \\ \ddot{y} = a_y - \omega^2 y \\ \ddot{z} = a_z - 2\omega\dot{x} + 3\omega^2 z \end{cases} \tag{11}$$

Where $\rho\big|_{To} = R_{To} = [x, y, z]^T$, $\Delta a\big|_{To} = [a_x, a_y, a_z]^T$, ω is the target spacecraft orbit angle rate.

During space robot approaching target spacecraft in the final phase, target spacecraft operates the orbit maneuver in a general way. So, $\Delta a\big|_{To}$ can be rewritten as

$$\Delta a\big|_{To} = \Delta a_d\big|_{To} + u_C\big|_{To} \tag{12}$$

Where $\Delta a_d\big|_{To}$ expresses the differential disturbance and $u_C\big|_{To}$ expresses space robotic orbit maneuver acceleration.

The C-W equations can be written with matrix expression

$$\dot{X} = AX + BU + w \tag{13}$$

The discrete-time process is governed by the linear stochastic difference equation

$$X(k+1) = A_d X(k) + B_d U(k) + w(k) \tag{14}$$

Where A and B are known constant matrix, U is space robotic orbit maneuver acceleration in robot LVLH frame, w which is decided by disturbance source and relative distance between satellites is regarded as system noise. A_d, B_d are discrete with t, $X(k)$ denotes the value of X in k.

IV. RELATIVE NAVIGATION ALGORITHM

Combining the state equations and the observation equation which have been derived above, in this section, we design the relative navigation algorithm in detail. These discrete equations are rewritten below

$$X(k+1) = A_d X(k) + B_d U(k) + w(k) \tag{15}$$

$$Y_{new}(k) = H \cdot X(k) + s_{new}(k) \tag{16}$$

The random variable $w(k)$ and $s_{new}(k)$ represent the process and measurement noise respectively. $w(k)$ derives the higher order gravitational potential terms and the periodic environment forces, it can be analyzed and regarded as zero mean value approximately. $s_{new}(k)$ is correlative with measure value of optical sensor. After testing and calibration, we can obtain the probability statistic value also. They are assumed independent each other, white, and with normal probability distributions.

$$p(w) \sim N(0, Q) \tag{17}$$

$$p(s_{new}) \sim N(0, R) \tag{18}$$

The process noise covariance Q and measurement noise covariance R matrices might change with each time step, however we assure they are constant here.

Based on the white noise and zero mean value presupposition, the linear Kalman filter can be used to estimate optimally linear system states. Limited by paper length, this paper omits the expatiation. The Kalman filter need operate a inversion of 6×6 matrix and a lot of multiplication. It's profitable to find out a simply algorithm based on the filter. We know that, in the first some time, the gain which is derived by filter is changeful. However, it will tend to a constant gradually by time. So, a constant gain is considered below.

Giving the Riccati equation as follows

$$A_d P + P A_d{}^T - P H^T R^{-1} H P + Q = 0 \tag{19}$$

Where P is the convergent covariance matrix of linear Kalman filter. Other matrixes are known constant in (19), so it's easy to solve the matrix P. Following, the convergent gain can be derived by

$$K = R^{-1} H^T P \tag{20}$$

At last, a simplified constant gain linear Kalman filter is obtained below:

$$\tilde{X}(k+1) = A_d \tilde{X}(k) + K \cdot (Y_{new}(k+1) - \hat{X}(k+1)) \qquad (21)$$

Where $\tilde{X}(k+1)$ is the estimation of system state in $k+1$, and $\hat{X}(k+1)$ is the state prediction based on the time update equations

$$\hat{X}(k+1) = A_d \tilde{X}(k) + B_d U(k) \qquad (22)$$

According to linear system observability theory, the observation matrix can be derived

$$\Phi = A_d - KH \qquad (23)$$

The poles of matrix Φ can reflect the performance of filter. Namely, it's easy to obtain the response characteristic and damping coefficient each state. If some pole is much closer or removed to virtual axis, It will be improved by modifying the gain K correspondingly. At last, we may find out the balance between optimal estimation and response rate.

V. APPRAOCHING OPERATIONS TEST BED

This section will introduce an approaching operation test bed which is used to test the relative navigation algorithm above. As some other simulation platform [9-11], the test bed is designed as hardware-in-loop simulator offering the capability of real-time, real-size and real-motion simulation combined with optics sensor system [12].

The test bed can simulate the full 6-degrees of freedom (6-DOF) relative motion of two spacecraft in neighboring orbits. It consists of six parts.

- Part 1: Attitude and relative position simulation platform of chase spacecraft. It can be driven from the dynamics simulation data to operate 3-axis positions and 3-axis attitudes motion. The 3-axis position ranges are 12m, 3m and 1.8m respectively. The 3-axis attitude ranges are ±10º.
- Part 2: Attitude simulation platform of target spacecraft. It consists of a platform mounted 6-DOF industrial manipulator and a target spacecraft model. The 3-axis attitudes of target spacecraft model can rotate via operating manipulator.
- Part 3: Real-time numeric simulation system. Based on an industrial computer, it realizes several numeric simulation modules and the interfaces to other equipment outside. The main software modules include chase spacecraft orbit and attitude dynamics simulation, target spacecraft orbit and attitude dynamics simulation, target spacecraft attitude controller, and relative motion calculation between spacecrafts.
- Part 4: Optical sensor system. It consists of the optical sensor fixed on part 1 and the marker fixed on part 2. Screened image data of markers are transferred to the processor in ground.
- Part 5: Guidance, Navigation and Control (GNC) of chase spacecraft. It receives the measure information and sends control signal to numeric simulation system.
- Part 6: Display and control system in ground.

The configuration sketch map of the test bed is shown in Fig. 3, and the physical photo is shown in Fig. 4.

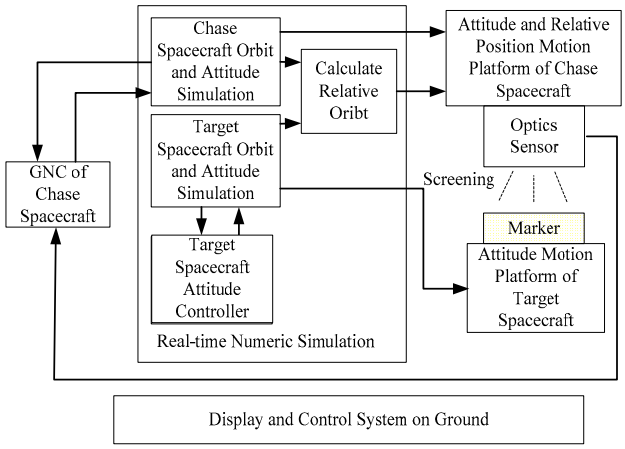

Figure 3. The configuration of the test bed

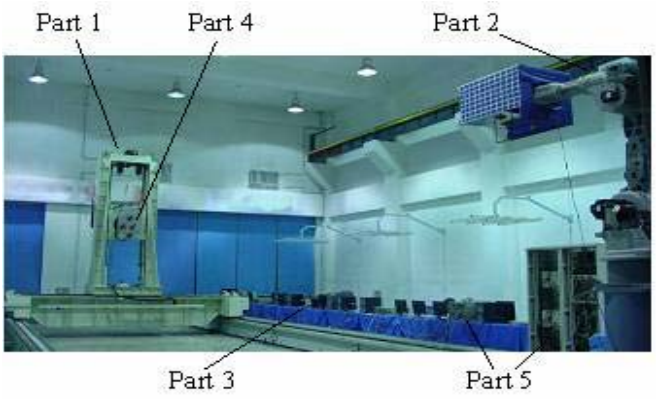

Figure 4. Pysical photo of the test bed

The physical device of optical sensor system is shown in Fig. 5. It consists of UP680 CCD camera made by UNIQ and M1614 lens made by Computar company. Additionally, a light filter is covered in front of lens. The marker consists of 3 big LED sources and 3 small ones to adapt different work distances.

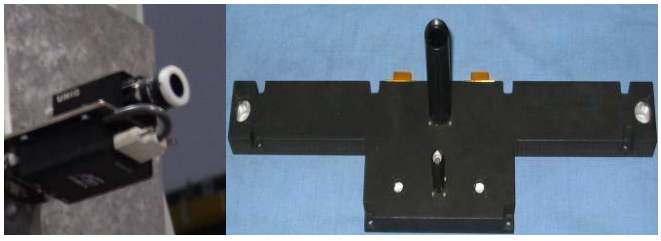

Figure 5. Physical photo of optical sensor system

VI. EXPERIMENT STUDY

The preceding relative navigation algorithm is dynamically validated below for different relative position. In this section, a relative motion task of space robot serving on orbit is designed. The various steps involved in the simulation are as follows:

- Step 1: Initial station keeping in 12m point which is the beginning position of final proximity phase.
- Step 2: Approaching 2m with the line of sight guidance.
- Step 3: Station keeping in 2m point which is the berthing position of space robot serving on orbit.
- Step 4: Retreating to 12m finally.

The actual initial condition for the space robot relative to the target spacecraft expressed in the LVLH frame of target spacecraft is given.

$$[x_0, y_0, z_0] = [-11.9, 0.1, -0.1]m ,$$

$$[\dot{x}_0, \dot{y}_0, \dot{z}_0] = [-0.01, 0.005, -0.001]m/s .$$

Space robot actual initial attitude and angle rate bias to its LVLH frame is given.

$$[a_{x0}, a_{y0}, a_{z0}] = [0, 0, 0]^\circ ,$$

$$[\dot{a}_{x0}, \dot{a}_{y0}, \dot{a}_{z0}] = [-0.2, 0.2, 0.2]^\circ / s$$

Fig. 6 and Fig. 7 show typical simulation result with relative position and velocity curves respectively. It's obvious that space robot has realized the approaching, berthing and retreating to target spacecraft by programming. The curves in Fig. 8 shows space robot attitude bias with its LVLH frame. The error curves of relative navigation are shown in Fig. 9 and Fig. 10.

Now, we analyze the curves of Fig. 9 and Fig. 10 in detail. All three components of the relative position navigation errors are no bigger than 5cm and velocity ones are less than 6mm/s. The navigation precision of x-axis is worse because of the bigger measure bias and noise of optics sensor in this direction. The maximal errors occur in the phase of accelerating and decelerating. During station keeping or moving with approximate constant velocity in x-axis, relative navigation works well. In stable state, the precision is 2cm in position and 2mm/s in velocity during far section (12m), and it's much higher in the near section (2m) about millimeter-level and less than millimeter/s-level.

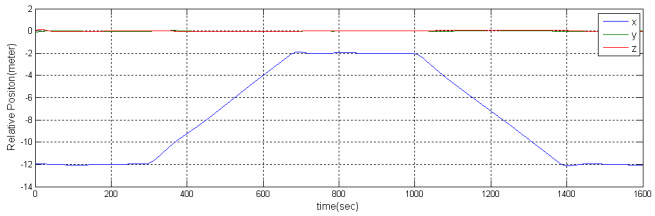

Figure 6. Relative position curve between spacecrafts

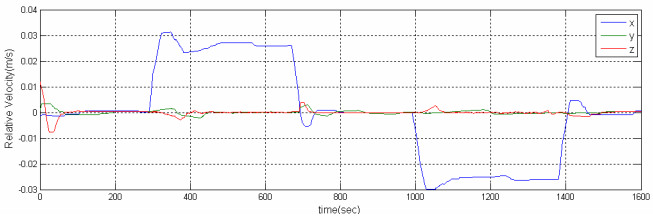

Figure 7. Relative velocity curve between spacecrafts

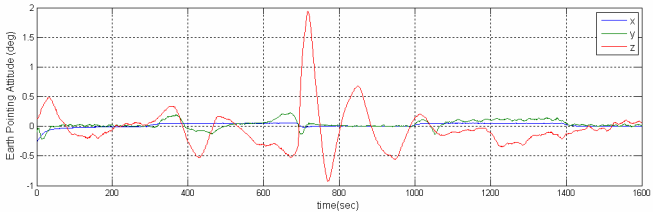

Figure 8. Space robotic attitude curve in LVLH frame

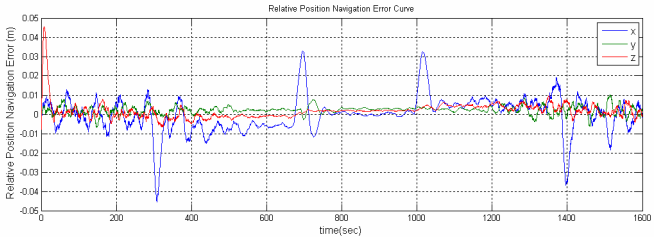

Figure 9. Relative position navigation error curve

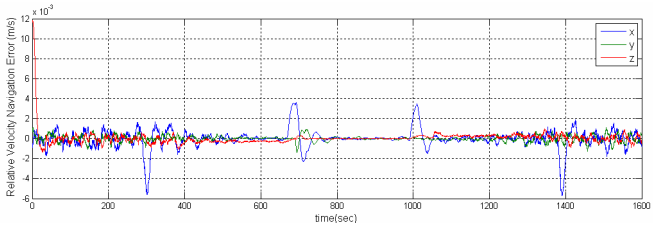

Figure 10. Relative velocity navigation error curve

VII. CONCLUSION

A relative navigation scheme for the final approach phase is proposed, with the target spacecraft information measured by optical sensor. A linear Kalman filter used to relative navigation is designed with constant gain, combining the relative motion dynamics (between two spacecrafts) with the measure principle of optimal sensor. At the same time, the attitude bias and fix bias is treated by relative navigation algorithm. The dynamic performance of the filter is theoretically analyzed according to the positions of its poles.

A hardware-in-loop simulation has operated in the test bed to test the algorithm. The result shows, in the initial position of final approach phase (about 12m), the precisions of relative position and velocity are centimeter-level and millimeter/s-level, and in the final berth (about 2m), the precisions are less. It will be accurate enough to satisfy the requirement of space robot's orbit controller. On the other hand, the relative navigation can stabilize quickly. As a result, the algorithm will be helpful to the GNC design of space robot.

However, some additional factors should be considered in practice. Firstly, the real time is important especially during the final approaching phase, but the relative measure data obtaining from optical sensor is earlier than the current navigation time (larger than 0.2s usually) because of the screening time, the image processing time and the communication time. A feasible method is compensating the delay via state forecast. The second, Fig. 9 and Fig. 10 show large relative navigation error in the phase of accelerating and decelerating, so a kind of accurate accelerometer is helpful to improve navigation performance. Some of these topics will be addressed in the future.

REFERENCES

[1] Oda, M. Kibe, K and Yamagata, F. ETS-VII, space robot in-orbit experiment satellite[C]. Robotics and Automation, 1996. Proceedings. Minneapolis, MN, USA. vol.1, 739-744.

[2] David C. Woffinden, David K. Geller. Navigating the road to autonomous orbital rendezvous.[J] Journal of spacecraft and rockets, 2007. Vol. 44(4): 898~909.

[3] F. Busse, J. How. Real-time experimental demonstration of precise decentralized relative navigation for formation flying spacecraft[C]. AIAA Guidance, Navigation, and Control Conference and Exhibit, Monterey, California, Aug. 5-8, 2002

[4] Howard, R.T.; Bryan, T.C.; Book, M.L. An advanced sensor for automated docking[C]. DASC. The 20th Conference. Volume 2, 14-18 Oct. 2001

[5] Roberto Alonso, John L. Crassidis and John L. Junkins. Vision-based relative navigation for formation flying of spacecraft. AIAA Guidance, Navigation, and Control Conference and Exhibit[C]. Denver, CO, Aug. 14-17, 2000

[6] Son-Goo Kim, John L. Crassidis, Yang Cheng, Adam M. Fosbury and John L. Junkins. Kalman Filtering for Relative Spacecraft Attitude and Position estimation[J]. Journal of Guidance, Control, and Dynamics 2007, vol.30 no.1, 133-143

[7] N.K. Philip and M.R. Aanthasayanam. Relative position and attitude estimation and control schemes for the final phase of an autonomous docking mission of spacecraft[J]. Acta Astronautica, 2003, 52, pp 511-522.

[8] M. Monda and H. Schaub. Spacecraft Relative Motion Estimation using Visual Sensing Techniques[C]. Infotech@Aerospace, Arlington, Virginia, Sep. 26-29, 2005

[9] Fehse. W. Automated Rendezvous and Docking of Spacecraft, Cambridge aerospace series[M]. Washington DC, 2003.

[10] R. Bell, T. Morphopoulos, J. Pollack, J. Collins, JR Wertz and RE Van Allen. Hardware-in-the-Loop Tests Of An Autonomous GN&C System for On-Orbit Servicing[C]. AIAA Responsive Space Conference, 2003

[11] Toralf Boge, Erwin Schreutelkamp. A new commanding and control environment for rendezvous and docking simulations at the EPOS-facility[C]. SESP, ESTEC, Noordwijk, 12-14 November, 2002

[12] Weinan Xie, Guangcheng Ma, Qiyong Wen and Hongwei Xia. A ground semi-physical simulator for satellite autonomous rendezvous and space robot capture[C]. ISSCAA 2006. Harbin